Therapeutic and imaging potential of peptide agents in cardiocascular disease

Yu, H.

3

Atherosclerosis Imaging Potential of a Novel Peptide Ligand selective for SR-AI

Haixiang Yu*, Filip Segers*, Perry Prince, Toshiki Tanaka†, Theo J.C. van Berkel*, and Erik A.L. Biessen*‡

*Division of Biopharmaceutics, Leiden/Amsterdam Center for Drug Research, Leiden University, Leiden, the Netherlands. † Department of Material Science, Graduate School of Engineering, Nagoya Institute of Technology, Gokiso-chou, Nagoya, 466-8555, Japan.

Running title: Peptide Antagonist Specific for Scavenger Receptor A

Abstract

***Objective*—**Macrophage scavenger receptor A (SR-A) is mainly expressed by macrophages and plays a critical role in foam cell formation and atherosclerosis. In search of antagonist specific for SR-AI, we have employed affinity selection of a random phage displayed peptide library on a synthetic receptor comprising the ligand binding site.

***Methods and Results*—** Phage selection led to enrichment of SR-AI binding phage. The selected phage pool bound avidly to human THP-1 and moderately to murine RAW 264.7 macrophages, and binding could be displaced by polyinosinic acid and succinylated human serum albumin. A synthetic peptide sequence encoded by the major SR-AI binding phage clone (PP1) was able to displace ligand binding to SR-AI at an IC_{50} of 29 μM and the minimal essential motif required for SR-AI interaction was defined. After docking to a streptavidin scaffold, peptides were effectively internalized by macrophages in a SR-AI dependent manner. The enriched phage pool and streptavidin immobilized PP1 exhibited a similar in vivo biodistribution profile in mice with marked accumulation in hepatic macrophages. Importantly, PP1 affected a significant 2-fold increase of ^{125}I-streptavidin uptake by aortic artery lesions in ApoE$^{-/-}$ mice, which was not observed for the control.

***Conclusions*—** We have identified a specific peptide antagonist for SR-AI by peptide phage display on a synthetic receptor fragment, which proved effective in SR-AI targeted imaging of atherosclerotic lesions.

Introduction

Macrophages play a key role in atherosclerosis at all stages of disease development. Type A scavenger receptors (SR-A) have been implicated in atherosclerosis lesion formation and mediate the uptake of modified low density lipoproteins (LDL)[1-3]. SR-A is a trimeric transmembrane glycoprotein consisting of 6 distinct domains[4,5] and can exist in one of three isoforms (SR-AI, SR-AII and SRA-III) [6,7]. As pattern recognition receptor, it displays a very broad substrate profile, internalizing modified LDL, polyinosinic acid (poly I), polysaccharides fucoidan and lipopolysaccharide (LPS) [8-10]. SR-A is mainly expressed by liver macrophages but also by liver endothelial cells[11]. In addition, SR-A was found to be abundantly expressed by macrophages, foam cells and smooth muscle cells[12] in atherosclerotic lesions but not in the normal vessel wall[13,14]. The involvement of SR-A in atherogenesis was first established by Suzuki *et al*[15] showing that lesion formation was reduced in SR-A-deficient ApoE$^{-/-}$ compared to ApoE $^{-/-}$ control mice. Subsequent studies were in support of this notion[16].

The marked SR-AI expression and inflammation in macrophage enriched sites of atherosclerotic lesions and the fact that this receptor mediates the efficient endocytosis of its substrates indicates that SR-AI may not only be an interesting target for therapeutic intervention in atherosclerosis and inflammation but also for targeted drug delivery and imaging approaches. Importantly, SR-AI expression is associated with newly invaded macrophages in the atheroma, which are particularly prominent in vulnerable plaques[17]. Application of selective SR-AI ligands as homing device for contrast agents may therefore not only improve the sensitivity of atherosclerotic plaque imaging but also may give insight into the actual composition and stability of the plaque.

Given the complex chemical nature of the macromolecular substrates for SR-AI it is not surprising that ligand design for this receptor has not been very successful and has only resulted in a single report on a synthetic rather unselective SR-A antagonist [18]. In this study, we describe the unbiased design of SR-AI antagonists involving the use of phage display on a synthetic receptor comprising the actual ligand-binding pocket of SR-AI. A selective peptide antagonist for SR-AI was identified, which constitutes a promising lead to the development of SR-AI targeted therapy and imaging of atherosclerotic lesions.

Materials and Methods

Phage library

The pComb3 phage displayed peptide library X15 (in which X is any amino acid) was generated by Dr Pannekoek and co-workers (University of Amsterdam, the Netherlands).

Peptide synthesis

All peptides were synthesized on an automated peptide synthesizer (9050 Millipore, MA) using standard Fmoc solid-phase peptide synthesis. Crude peptides were purified on a preparative C_8 RP-HPLC column (Altech, Deerfield, IL) using a

JASCO PU-980 (Tokyo, Japan). Purified peptides were further characterized by LC-MS in Division of Analytical Biosciences, Leiden University. The purity of the peptide, as checked by MALDI-TOF mass spectrometry and RP-HPLC, was at least 70%. Biotinylated PP1 peptide LSLERFLRCWSDAPAK-biotin (BioPP1) was more than 95% pure. Lyophilized peptides were stored at -20ºC under nitrogen until further use. Synthetic biotinylated bovine SR-AI was synthesized, purified and characterised as described by Suzuki et al[19].

Selection of SR-AI binding phage

10 μg/mL of streptavidin in coating buffer (50 mM NaHCO3, pH 9.6) was incubated overnight at 4ºC in a high binding 96 well plate (Costar, Corning, UK) at 100 μL/well. Subsequently, wells were washed with assay buffer (20 mM HEPES, 150 mM NaCl, 1 mM CaCl2, pH 7.4) and incubated for 1 h at 37ºC with blocking buffer (3% BSA in assay buffer). After washing, wells were incubated with 50 μM of biotinylated SR-AI (2 h 37ºC), washed, and subsequently incubated for 2 hours at room temperature (RT) with the phage libraries at 10^9 colony forming units (CFU) in 100 μL of binding buffer (0.1% BSA, 0.5% Tween 20 in assay buffer). Wells were washed 10x with binding buffer and binding phage were eluted by incubation for 5 min at RT with 100 μL of elution buffer (0.1 M glycine/HCl, pH 2.2) and neutralized by addition of 50 μL of neutralization buffer (1 M Tris/HCl, pH 8.5). Phage were titrated, amplified and purified as described[20]. Amplified phage was used for further selection. For DNA sequencing of enriched phage pools, plasmid DNA was isolated from single colonies using the Wizard plus SV Miniprep DNA Purification System (Promega, Madison, USA). DNA sequencing was conducted at the DNA-sequencing facility of the Leiden University Medical Center using a standard M13 primer. Unless otherwise stated, the amplified phage pool of round 7 was used for further characterization experiments.

Cell culture

Murine macrophage cells (RAW 264.7), African green monkey kidney COS-7 and human monocytic THP-1 cells were grown in Dulbecco's Modified Eagles's Medium (DMEM) supplemented with 10% (v/v) heat-inactivated foetal bovine serum (FBS), 100 units/mL penicillin, and 100 μg/mL streptomycin. Bone marrow derived macrophages were isolated from C57BL/6 mice and cultured as described before[21]. Cell cultures were maintained at 37 ºC in humidified 95% air/5% CO2.

Cell binding assay

COS-7 and RAW 264.7 cells were grown to approximately 60~70% confluency in 12 wells plates, while non-adherent THP-1 cells were grown to $4 \cdot 10^5$ cells/well. Cells were pre-incubated in DMEM+0.2% BSA, 2h at 37°C. SR-AI specific phage (round 7) was added at a titer of 10^8 CFU and incubated for 2h at 4°C. Non-selected phage library was used as a negative control. RAW and COS-7 cells were washed 10x with PBS and lysis buffer (500 μL Reporter E397A, Promega, Madison, USA) was added. The THP-1 cell suspension was washed 10x with PBS, subsequently centrifuged for 5 min at 10,000 rpm and the cell pellet was resuspended in PBS. Finally, cells were lysed by addition of 500 μL lysis buffer.

Input samples were taken from the incubation medium immediately after addition of the phage and diluted 1:100 in 1x Tris Buffered Saline (TBS) in a total volume of 1 mL. Output samples were taken from the cell lysate and diluted 1:10 or 1:100 (total volume: 500 µL). The recovery of bound phage was calculated from the output to input ratio.

Competition experiment of SR-AI selected phage pool

In analogy to the phage selection conditions, streptavidin (10 µg/mL in coating buffer) was incubated overnight at 4ºC in a high-binding 96-well plate at 100 µL/well. Wells were washed 3x with assay buffer and incubated for 1 h at 37ºC with blocking buffer. Next, wells were incubated for 2h at 37°C with 125 nM biotininylated SR-AI binding peptide (100 µL/well), washed 3x with binding buffer, after which SR-AI ligands or synthetic SR-AI peptides (full length or N-terminal truncations of 7, 9, 11, 13 amino acids) were added and the solution (100 µL) was left to incubate for 2h at RT with the enriched phage pool (round 7) at 10^8 cfu. Wells were washed 10x with binding buffer, binding phage were eluted by incubation for 5 min at RT with 100 µL elution buffer, and neutralized with 50 µL neutralization buffer (1M Tris-HCl, pH 8.5). Residual phage binding was calculated from the output ratio.

***In vivo* distribution of SR-AI selective phage pool**

SR-AI specific PP1 phage and a non-selected control phage were radiolabeled as previously described[20] and injected at 10^9 CFU (~200,000 DPM) via the tail vein into anesthetized C57BL/6 mice (20 weeks old male; n=6). After 30 min, mice were perfused for 2 min with DMEM at 10 mL/min via a cannula inserted in the left ventricle. Organs were removed, weighed and organ homogenates were obtained by overnight incubation of ~0.1g tissue with 500 µL Solvable at 56ºC (Packard bioscience, Groningen, the Netherlands) and analyzed for associated ^{35}S radioactivity in a beta counter after adding 15 mL Hi-ionic Fluor (Perkin-Elmer, Boston, USA) .

PP1 docking to streptavidin

To monitor optimal occupation of the available biotin binding sites, streptavidin (Amersham, Little Chalfont, UK) was incubated for 30 min at room temperature with bio-PP1 at the indicated molar ratio in the presence of an excess amount of ^3H labeled biotin (~200, 000 DPM; Amersham). The mixture was then chromatographed over a Sephadex G-50 medium (Amersham) column (5 mL), eluting with PBS and 500 µL fractions were collected. Samples were analyzed for radioactivity on a beta-counter after adding 4.5 mL Hi-ionic Fluor (Perkin-Elmer, Boston, USA) .

PP1 peptide specifically binds to macrophage SR-AI

Bone marrow derived macrophages were matured by incubation with 20 µg/mL oxidized LDL overnight in a 9 cm petri dish. Adherent cells were detached by adding 3 mL 4 mM EDTA. Cells were collected, centrifuged and washed with ice-cold PBS (4ºC). The resuspended cells were incubated at 37ºC in the dark in complete DMEM with 40 nM of streptavidin-PE, strepPE-bioPP1 or strepPE-

bioPP1 premixed with 1 mg/mL fucoidan (Sigma, St. Louis, USA). After incubation with DAPI working solution (Molecular Probes, USA) for 30 min at room temperature, cells were washed and cytospins (300 rpm, 5 min) were performed, mounted to the coverslip with fluorescent mounting medium (DAKO, Denmark) and analyzed under fluorescent microscope.

Displacement studies of PP1 binding to RAW 264.7 cells

Freshly prepared 0.38 nM ^{125}I Strep-bioPP1 was incubated with murine RAW 264.7 cells for 1h at 37^{o}C in a 12-well plate (400,000/well) in the presence of fucoidan at the indicated concentrations. Cells were subsequently washed three times with 1mL ice-cold 1xTBS/0.2% BSA (bovine serum albumin, pH7.4), and three times with 1mL ice cold TBS and then lysed in 500 µL 0.1M NaOH. The radioactivity of the cell lysate was measured in a gamma counter.

***In vivo* organ distribution studies**

C57Bl/6 mice (n=6; male, 20 weeks) were intravenously injected with 0.38 nM freshly prepared ^{125}I strep-biotin or ^{125}I strep-bioPP1 in 100 µL of 0.9% sodium chloride. After 1h, mice were sacrificed, organs were removed and weighed, and the entrapped radioactivity was counted in a gamma counter.

PP1 peptide selectively target to the atherosclerotic lesions

Aged ApoE$^{-/-}$ mice (> 65 weeks, male, weight 30±2g, fed a chow diet) with advanced atherosclerotic lesions were intravenously injected with ^{125}I strep-biotin or ^{125}I strep-bioPP1 (0.38 nM, n=3). Mice were sacrificed 1h after injection, perfused via a left ventricle cannula with PBS and fixed with 4% formaldehyde. The aorta was isolated, stained for lipids with Oil Red O using a routine protocol and subjected to autoradiography, exposing it to a phosphor screen at room temperature for one week. The intensity of the signal was quantified by ImageQuant software (Bio-Rad, USA), and the results were expressed as percentage of the maximum signal obtained in the ^{125}I strep-bioPP1 treated group. The oil red-O-stained image was quantified and expressed as percentage of stained area of total aorta.

Statistical Analysis and animal handling ethics

Values are expressed as mean ± SEM. A two-tailed unpaired Student's t-test was used to compare individual groups. A level of $P<0.05$ was considered significant. Animal experiments were performed at the Gorlaeus laboratories of the Leiden/Amsterdam Center for Drug Research in accordance with the National Laws. All experimental protocols were approved by the Ethics Committee for Animal Experiments of Leiden University.

RESULTS

Selection of SR-AI binding phage

A 15 amino acid random phage displayed peptide library was screened for SR-AI binding peptide ligands. To favor the selection of peptides binding to the actual binding pocket of SR-AI, biopanning was performed on wells coated with a streptavidin associated biotinylated peptide encompassing the complete ligand

binding motif of SR-AI[19]. In the first two rounds a non-stringent washing protocol with ice-cold binding buffer was used, while from round three onwards stringency was gradually increased by decreasing the coating density of synthetic SR-AI and by using a non-cooled binding buffer for washing. This led to a 500-fold enrichment of binding phage in the 5th round (Fig.1A). Subsequent DNA sequence analysis of 10 phage clones from the 6th and 7th selection round revealed a 12-mer consensus motif. 8/10 phage clones from round 6 shared the peptide sequence LSLERFLRCWSDAPA (PP1) while 2/10 clones carried a highly homologous LSLERFLRCWSDSPR (PP2) insert. In 7th round, only PP1 clones were detected suggesting that PP1 phage was more effectively bound than PP2. Compared with the parental non-selected phage library, the enriched phage pool showed high binding to streptavidin immobilized SR-AI peptide but only marginal binding to streptavidin immobilized biotin or to type-2 collagen S. There was no binding of the non-specific phage to streptavidin immobilized SR-AI, confirming that binding of the selected phage pool implicated the SR-AI moiety (Fig.1B).

Cell binding of the enriched phage pool

To verify whether the selected phage pool (PP1) was also able to bind to the full-length receptor on macrophages, we have tested the ability of the phage pool binding to human THP-1 and murine RAW cells, which were shown to display SR-AI expression. Compared to the parental phage library, the selected phage avindly bound to human THP-1 cells (Fig.1C) and to a lesser extent to murine RAW cells, although RAW binding still was >2-fold higher than that to monkey COS-7 cells, which are deficient in SR-AI.

Competition assay of phage binding to SR-AI by established SR-AI inhibitors

To further characterize the specificity and the affinity of the selected phage binding, displacement studies of phage binding to SR-AI by the established SR-AI inhibitors poly I and suc-HSA were performed. Both poly I (IC_{50}=10.5 μg/mL) and suc-HSA (IC_{50}=66 μg/mL) was able to dose-dependently compete for phage binding to SR-AI (Fig.1D).

Competition assay of phage binding to SR-AI by synthetic peptides

DNA sequence analysis revealed the presence of a 12-mer consensus sequence within the peptide insert of the PP1/PP2 phage clones, suggesting the N-terminal part of the phage encoded peptide to be instrumental in SR-AI binding. To pinpoint the minimal peptide sequence required for SR-AI binding we have performed a truncation study. At which we focused on the N-terminal of the peptide. Full-length peptide LSLERFLRCWSDAPA (PP1) and truncated peptides LERFLRCWSDAPA (PP1-13), RFLRCWSDAPA (PP1-11), LRCWSDAPA (PP1-9) and CWSDAPA (PP1-7) were synthesized with Fmoc chemistry. The capacity of the peptides to interfere with phage binding to SR-AI was tested in a competition assay at which residual binding of the selected phage to SR-AI was determined in the presence of the synthetic peptides (Fig.2). It appears that PP1 could dose-dependently and potently inhibit SR-AI binding of the enriched phage at an IC_{50} value of 29 μM. Stepwise truncation of PP1 resulted in a gradual

reduction of the affinity of the peptide, and the 11-mer peptide PP1-11 was identified as the minimal motif of PP1 to bind to SR-AI.

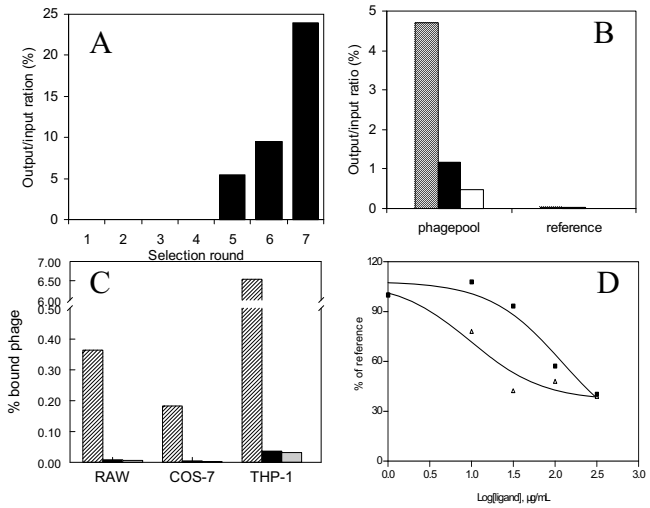

Figure 1 Selection and specificity of SR-AI binding phage. (A) Selection of the pComb3 X_{15} phage displayed peptide library on immobilized synthetic biotinylated SR-AI resulted in a sharp enrichment of SR-AI binding phage from the 5th round of selection onwards (up to 918-fold in the 7th round). **(B)** The enriched phage pool specifically bound to biotinylated SR-AI peptide (hatched bars) but not to streptavidin immobilized biotin (black/filled bars) or collagen S (open bars). As a reference, non-specific phage pool showed little binding to SR-AI. Values are expressed as ratio of output/input ratio and represent means of duplicate experiments. **(C)** Enriched phage pool (hatched bars) but not the parental library (WT; black bars) and the controlled nonspecific phage library (open bars) displayed avid binding to human THP-1 cells, moderate binding to murine RAW cells and only poor binding to COS-7 cells. Values are expressed as output/input ratio and are means of two independent experiments. (D) Binding of the enriched phage pool to biotinylated SR-AI was determined in the presence of Suc-HSA (■) or poly I (Δ).IC_{50} values, as calculated from the competition curves were 66 µg/mL and 10.5 µg/mL, respectively. Values are expressed as percentage of total phage binding in the absence of the inhibitors and represent means of two independent experiments.

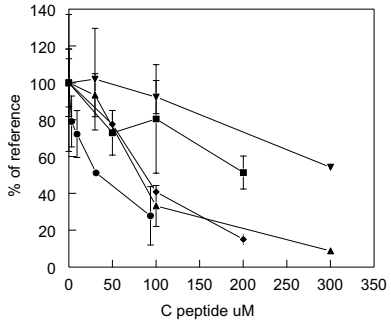

Figure 2 Competition of SR-AI specific phage binding to synthetic SR-AI by synthetic PP1 or trunctated analogues thereof. Binding of the enriched phage pool to synthetic SR-AI was determined in the presence of 0-300 µM of LSLERFLRCWSDAPA (●), LERFLRCWSDAPA (▲), RFLRCWSDAPA (♦), LRCWSDAPA (■), CWSDAPA (▼). Values are expressed as a percentage of total binding in the absence of peptide and represent means of three independent experiments ±SD. The IC_{50} values as calculated from the displacement curves were 29.1 µM, 72.3 µM, 80.9 µM, uncalculated, and 217 µM, respectively.

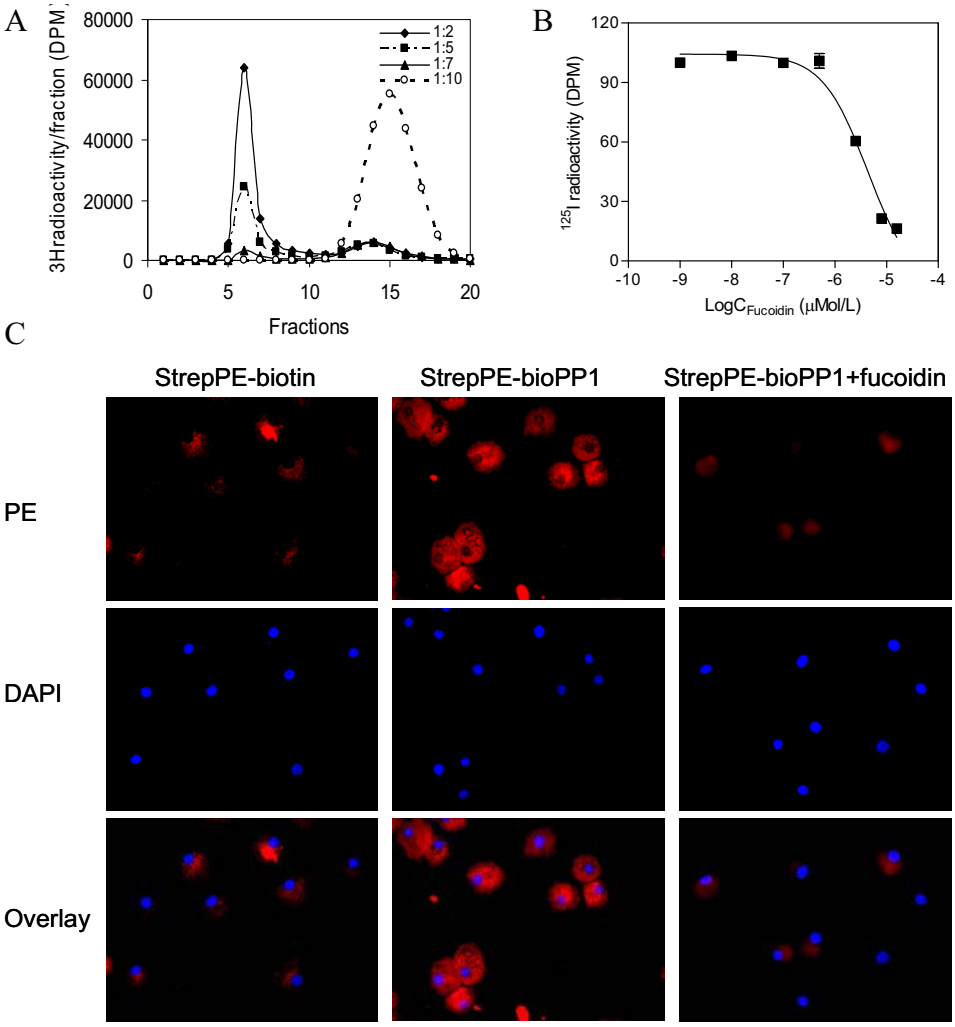

Figure 3 Streptavidin immobilized PP1 is internalized by macrophages in a SR-AI dependent fashion (A) Sephadex gel chromatography was used to determine the optimal ratio of streptavidin to bioPP1 (B) ^{125}I strep-bioPP1 was incubated with RAW 264.7 cells (approx. 4.10^5/well) in the presence of fucoidan at the indicated concentrations. The radioactivity of the bound radioligand was measured. Values represent means±SD of three individual experiments. (C) Bone marrow derived macrophages, grown in the presence of 20 µg/mL oxLDL, were incubated with strepPE-biotin, strepPE-bioPP1 or strepPE-bioPP1 pretreated with 1 mg/mL fucoidan. Representative microscopic views illustrate effective uptake of StrepPE-bioPP1 by macrophages which is prevented by pretreatment with fucoidan. Second and third rows show corresponding nuclear DAPI staining (blue) and DAPI/PE overlay, respectively.

PP1 peptide selectively binds to macrophage

As SR-AI acts as a trimer and hence was shown to display a preference for oligomers[22], we argued that the affinity of PP1 for SR-AI may benefit from tetrameric presentation on a streptavidin scaffold[23]. Additional advantage would be that streptavidin docking will favorably affect the pharmacokinetics in vivo. To this point we have incubated streptavidin with different molar ratio of biotinylated PP1 peptide to prepare tetrameric Strep-bioPP1 complexes. Sephadex gel chromatography revealed that a protein to peptide ratio of 1:5 was optimal for conjugation and led to occupation of most of the biotin binding sites on streptavidin (Fig. 3A). Fucoidan, a polyanionic substrate of SR-AI, dose-dependently inhibited ^{125}I strep-bioPP1 binding to RAW cells at an IC50 of 4.2 μM (Fig. 3B). To illustrate that strep-bioPP1 selectively binds to macrophages in a SR-AI dependent rather than passive manner, the binding of streptavidin-PE conjugated PP1 peptide to macrophages was investigated by immunocytochemistry. Bone marrow derived macrophages were cultured in culture medium supplemented with conditioned medium containing macrophage colony-stimulating factor (M-CSF), to induce differentiation of progenitors into functional macrophages with SR-AI overexpression. FACS analysis was used to confirm the purity of the macrophage mix (F4/80 positive>99%). When conjugated to the streptavidin scaffold PP1 was able to give significant uptake signal at concentrations as low as 40 nM. Furthermore, unlike strepPE-biotin, strepPE-bioPP1 specifically accumulated in macrophages (Fig.3). StrepPE-bioPP1 was localized both at the membrane and in the cytosol, suggesting that uptake was SR-AI mediated rather than adsorptive endocytosis. Binding and internalization of strepPE-bioPP1 was abrogated by pretreatment the cells with 1 mg/mL fucoidan which further proved the selectivity of PP1 to SR-AI.

Targeting of SR-AI selective phage and phage encoded peptide into liver

As SR-AI is mainly expressed by resident macrophages in various organs including liver[24], we have examined the capacity of PP1 phage and PP1 peptide to accumulate in the liver after intravenous injection in mice. The PP1 phage displayed a significant 2-fold increase in liver accumulation compared to control phage. Liver and spleen appeared to be the most prominent sites of uptake, whereas less phage could be recovered from the heart (Fig.4A). ^{125}I-Streptavidin conjugated PP1 showed a similar biodistribution pattern with again a substantial and 2-fold increased accumulation by liver (P=0.002), albeit that liver uptake of strep-bioPP1 was less pronounced than that of the PP1 phage (Fig. 4B**).**

PP1 peptide targets atherosclerotic aortic artery lesions in ApoE$^{-/-}$ mice

Since SR-AI was found to be considerably overexpressed in atherosclerotic lesions *in vivo*, we have examined whether PP1 peptide would be able to target the aortic artery lesions of ApoE$^{-/-}$ mice. Relative lesion size was evaluated as percentage of Oil Red O stained area in the aorta as shown in Fig.5. The mean relative lesion area was approximately 50%, reflecting the advanced stage of lesion development in these aged mice. Importantly, plaque size in both treatment groups did not differ.

However, accumulation of radioactivity in aorta's after ^{125}I strep-bioPP1 injection was more than two-fold higher than that after injection of ^{125}I strep-biotin (P=0.007).

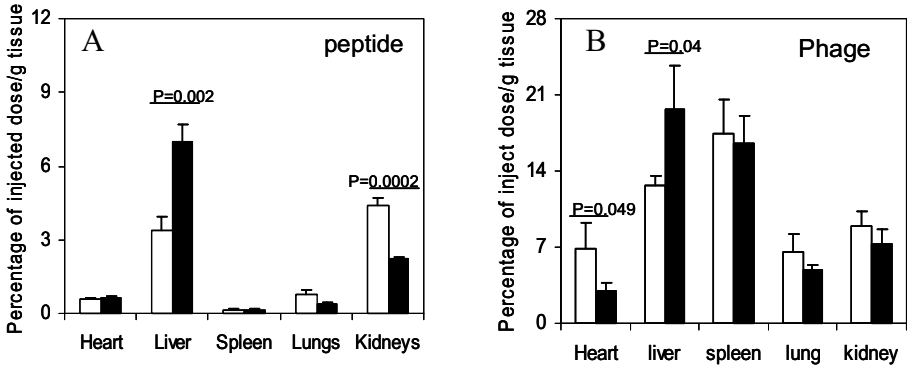

Figure 4 SR-AI binding phage as well as PP1 home to SR-AI rich tissue *in vivo* (A) ^{35}S labelled enriched phage (~200,000 DPM, black bars) and nonspecific control phage (200,000 DPM, open bars) were intravenously injected into C57Bl/6 mice. After 30 min circulation, organs were removed and the tissue distribution of radiolabled phage was determined as percentage of the injected dose/g tissue. (B) ^{125}I strep-biotin (open bars) or ^{125}I strep-bioPP1 (black bars) was intravenously injected to C57Bl/6 mice. After circulating for 1h, organs were isolated and the tissue distribution of radioligand was calculated as a percentage of the injected dose/g tissue. Values represent means ±SD of three individual experiments.

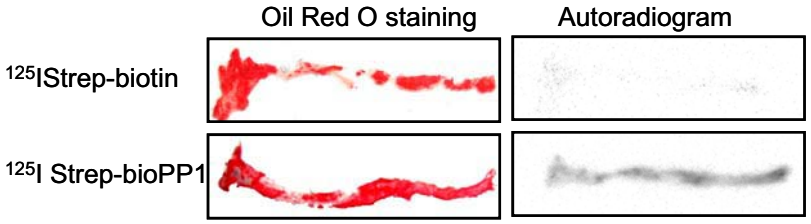

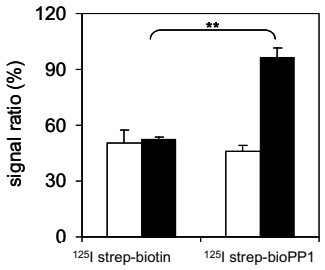

Figure 5 PP1 selectively targets atherosclerotic aortic artery lesions in ApoE$^{-/-}$ mice ^{125}I strep-biotin or ^{125}I strep-bioPP1 (0.38 nM) was intravenously injected into aged (>65 weeks) male ApoE$^{-/-}$ mice with advanced atherosclerosis (n=3). A representative Oil red O staining (upper left) and autoradiogram (upper right) of the aorta is shown. Relative lesion area (as a percentage of total aorta area; open bars) and the autoradiogram signal (as a percentage of the maximal signal in ^{125}I strep-BioPP1 treated group; black bars) are given in the lower panel (*: P<0.01).

Discussion

In search of potent and selective peptide antagonist binding to SR-AI we have employed phage display on a synthetic SR-AI receptor sequence. Phage display of randomized peptides library has evolved into a very powerful strategy for the unbiased selection of peptide ligands that bind to diverse targets[25]. The synthetic peptide encompassing the collagen-like binding domain of SR-AI allows to adopt a configuration and a ligand binding pattern that is very similar to that of SR-AI itself. This synthetic template is expected to bias the selection towards peptides that interact with the actual binding site of SR-AI and display antagonistic properties.

Selection appeared successful and led to the identification of SR-AI specific phage clones, with a shared 11-mer consensus motif in their insert. The C-terminus of the two peptides differed, suggesting that in particular the N-terminal part is relevant to SR-AI binding, which is congruent with the fact that in the phage display system peptides are fused at the C-terminal end to the coat protein (pIII). Protein BLAST search for short, nearly exact matches of PP1 revealed a highly homology of the N-terminal heptapeptide LSLERFL to viruses such as human cytomegalovirus (CMV) and HIV (Table 1), which both have been implicated in atherosclerosis.[26] As SR-AI was found to interact with gram-positive bacteria[10], it is tempting to assume that macrophage uptake of these pathogens is SR-AI mediated and proceeds through the LSLERFL motif. Further research will be required to establish the involvement of SR-AI in cellular uptake of the above infectious agents.

Table 1 Homology search by BLAST of PP1 peptide for short nearly exact matches

Sequence	Name and origin
LSLERFL	N-terminal part of isolated SR-AI selective binding phage
LALERFL	Envelope glycoprotein [Human immunodeficiency virus type 1]
SLERFL	Human herpes virus 5 [Cytomegalovirus]
SLERFL	Enterococcus faecium [Bacteria]

The peptide truncation studies revealed that deletion of up to four N-terminal amino acids was quite well tolerated in that the affinity of these truncated peptides for SR-AI was only slightly reduced. The enriched phage appeared to be very specific for SR-AI as it did not bind to polystyrene, collagen, or streptavidin immobilized biotin. Phage binding to SR-AI could be inhibited by established SR-AI inhibitors, suggesting that the phage clone indeed interacts with the collagen like ligand binding domain of SR-AI. The SR-AI binding phage not only bound avidly to the synthetic receptor but also to human THP-1 cells and, to a lesser extent, to murine RAW cells, which are both known to express high levels of SR-AI. The higher binding to THP-1 cells may be attributable to interspecies differences or to differences in SR-AI expression levels between the two cell lines as has previously been reported for P-selectin phage display[23]. Background binding of the selected phage to SR-AI deficient COS-7 cells was very low, which is a clear advantage when aiming at targeted delivery and imaging approaches *in vivo*.

In conclusion, a novel phage display strategy, based on biopanning for a synthetic peptide which encompasses the binding domain of the target receptor, was successfully applied for the design of SR-AI peptide antagonists. A 15-mer linear peptide lead was identified which is only 5-fold less potent than poly I, one of the most potent SR-AI inhibitors to date. Truncation studies firmly established the N-terminal part of the peptide as minimal essential motif required for SR-AI binding. Apart from its antagonistic capacity, the peptide was able to target SR-AI expressing cells in vitro and in vivo after docking to a streptavidin scaffold. Moreover, we demonstrate that the peptide was able to redirect an imaging device to atherosclerotic lesions in vivo. This lead may not only form the starting point for the design of even more potent SR-AI inhibitors but also prove useful in the development of imaging and targeting strategies aimed at macrophage enriched sites of inflammation such as the atherosclerotic plaque.

References

1. Van Berkel,T.J. *et al.* Scavenger receptors: friend or foe in atherosclerosis? *Curr. Opin. Lipidol.* **16**, 525-535 (2005).
2. Kunjathoor,V.V. *et al.* Scavenger receptors class A-I/II and CD36 are the principal receptors responsible for the uptake of modified low density lipoprotein leading to lipid loading in macrophages. *J. Biol. Chem.* **277**, 49982-49988 (2002).
3. Moore,K.J. & Freeman,M.W. Scavenger receptors in atherosclerosis: beyond lipid uptake. *Arterioscler. Thromb. Vasc. Biol.* **26**, 1702-1711 (2006).
4. Kodama,T. *et al.* Type I macrophage scavenger receptor contains alpha-helical and collagen-like coiled coils. *Nature* **343**, 531-535 (1990).
5. Rohrer,L., Freeman,M., Kodama,T., Penman,M. & Krieger,M. Coiled-coil fibrous domains mediate ligand binding by macrophage scavenger receptor type II. *Nature* **343**, 570-572 (1990).
6. Doi,T. *et al.* Charged collagen structure mediates the recognition of negatively charged macromolecules by macrophage scavenger receptors. *J. Biol. Chem.* **268**, 2126-2133 (1993).
7. Tanaka,T. *et al.* Synthetic collagen-like domain derived from the macrophage scavenger receptor binds acetylated low-density lipoprotein in vitro. *Protein Eng* **9**, 307-313 (1996).
8. Nagelkerke,J.F., Barto,K.P. & Van Berkel,T.J. In vivo and in vitro uptake and degradation of acetylated low density lipoprotein by rat liver endothelial, Kupffer, and parenchymal cells. *J. Biol. Chem.* **258**, 12221-12227 (1983).
9. Van Berkel,T.J., Van Velzen,A., Kruijt,J.K., Suzuki,H. & Kodama,T. Uptake and catabolism of modified LDL in scavenger-receptor class A type I/II knock-out mice. *Biochem. J.* **331 (Pt 1)**, 29-35 (1998).
10. Dunne,D.W., Resnick,D., Greenberg,J., Krieger,M. & Joiner,K.A. The type I macrophage scavenger receptor binds to gram-positive bacteria and recognizes lipoteichoic acid. *Proc. Natl. Acad. Sci. U. S. A* **91**, 1863-1867 (1994).

11. Daugherty,A., Cornicelli,J.A., Welch,K., Sendobry,S.M. & Rateri,D.L. Scavenger receptors are present on rabbit aortic endothelial cells in vivo. *Arterioscler. Thromb. Vasc. Biol.* **17**, 2369-2375 (1997).
12. Pitas,R.E. Expression of the acetyl low density lipoprotein receptor by rabbit fibroblasts and smooth muscle cells. Up-regulation by phorbol esters. *J. Biol. Chem.* **265**, 12722-12727 (1990).
13. Gough,P.J. *et al.* Analysis of macrophage scavenger receptor (SR-A) expression in human aortic atherosclerotic lesions. *Arterioscler. Thromb. Vasc. Biol.* **19**, 461-471 (1999).
14. de Winther,M.P., van Dijk,K.W., Havekes,L.M. & Hofker,M.H. Macrophage scavenger receptor class A: A multifunctional receptor in atherosclerosis. *Arterioscler. Thromb. Vasc. Biol.* **20**, 290-297 (2000).
15. Suzuki,H. *et al.* A role for macrophage scavenger receptors in atherosclerosis and susceptibility to infection. *Nature* **386**, 292-296 (1997).
16. Babaev,V.R. *et al.* Reduced atherosclerotic lesions in mice deficient for total or macrophage-specific expression of scavenger receptor-A. *Arterioscler. Thromb. Vasc. Biol.* **20**, 2593-2599 (2000).
17. Matsumoto,A. *et al.* Human macrophage scavenger receptors: primary structure, expression, and localization in atherosclerotic lesions. *Proc. Natl. Acad. Sci. U. S. A* **87**, 9133-9137 (1990).
18. Lysko,P.G., Weinstock,J., Webb,C.L., Brawner,M.E. & Elshourbagy,N.A. Identification of a small-molecule, nonpeptide macrophage scavenger receptor antagonist. *J. Pharmacol. Exp. Ther.* **289**, 1277-1285 (1999).
19. Suzuki,K., Yamada,T. & Tanaka,T. Role of the buried glutamate in the alpha-helical coiled coil domain of the macrophage scavenger receptor. *Biochemistry* **38**, 1751-1756 (1999).
20. Molenaar,T.J. *et al.* Uptake and processing of modified bacteriophage M13 in mice: implications for phage display. *Virology* **293**, 182-191 (2002).
21. Smookler,D.S. *et al.* Tissue inhibitor of metalloproteinase 3 regulates TNF-dependent systemic inflammation. *J. Immunol.* **176**, 721-725 (2006).
22. Pearson,A.M., Rich,A. & Krieger,M. Polynucleotide binding to macrophage scavenger receptors depends on the formation of base-quartet-stabilized four-stranded helices. *J. Biol. Chem.* **268**, 3546-3554 (1993).
23. Molenaar,T.J. *et al.* Specific inhibition of P-selectin-mediated cell adhesion by phage display-derived peptide antagonists. *Blood* **100**, 3570-3577 (2002).
24. Hughes,D.A., Fraser,I.P. & Gordon,S. Murine macrophage scavenger receptor: in vivo expression and function as receptor for macrophage adhesion in lymphoid and non-lymphoid organs. *Eur. J. Immunol.* **25**, 466-473 (1995).
25. Smith,G.P. & Petrenko,V.A. Phage Display. *Chem. Rev.* **97**, 391-410 (1997).
26. Ngeh,J., Anand,V. & Gupta,S. Chlamydia pneumoniae and atherosclerosis -- what we know and what we don't. *Clin. Microbiol. Infect.* **8**, 2-13 (2002).